Optimizing Free Carrier Absorption Measurements for Power Devices by Physically Rigorous Simulation

Robert Thalhammer

Infineon Technologies, WS SD D Tr, P. O. Box 80 09 49, D–81609 Munich,
Email: robert.thalhammer@infineon.com

Frank Hille, Gerhard Wachutka

Institute for Physics of Electrotechnology, Munich University of Technology

Abstract— **The carrier distribution in the interior of power devices can be determined from free carrier absorption measurements. In this work, a physically rigorous simulation of the entire measurement process is performed to investigate the effects which arise from the wave propagation of the probing beam and the sample preparation. Quantitative results for the optimization of the optical setup and the sample geometries which miminize the unavoidable experimental errors are presented.**

I. Introduction

Exploiting the dependence of the absorption coefficient α on the carrier concentration, the carrier distribution of the electron–hole plasma in the interior of forward conducting power devices have been ascertained by free carrier absorption measurements (cf. Fig. 1) [1], [2]. The injected carrier density $n(x)$ is extracted from the damping of the transmitted laser light intensity $I(x)$ during the on–state

$$\frac{I_{on}(x)}{I_{off}(x)} = \exp\left[-L\frac{\partial\alpha}{\partial C}\,n(x)\right] \qquad (1)$$

where L, $\partial\alpha/\partial C$, and $I_{on,off}$ denote the sample length, the dependence of the absorption coefficient on the injected carrier concentration, and the transmitted light intensity during on–state and off-state of the device under test, respectively.

However, evaluating the detector signal according to this simple absorption law does not take into account the surface recombination effects inevitably induced by the sample preparation. It also neglects the effects originating from the wave propagation of the probing beam during measurement, e. g. the lateral extension of the beam profile or the internal beam deflection due to temperature–induced gradients of the refractive index. In this work, all these effects are studied by a physically rigorous simulation of the entire measurement process.

II. Modeling Internal Laser Probing Techniques

A physically rigorous model for the simulation of internal laser probing techniques such as, e. g., free carrier absorption measurements has been developed [3] which accurately reflects the wave propagation of the probing beam through the sample and the experimental setup. Since the optically absorbed power of the probing beam is negligible compared with the electrical power dissipation of the device under test, we can

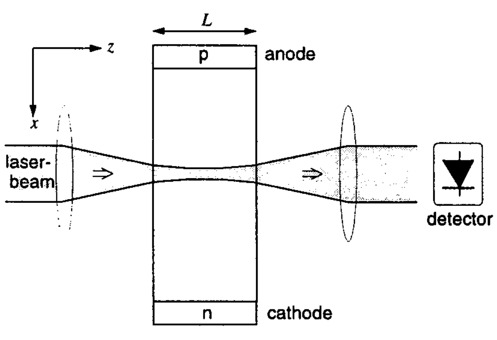

Fig. 1. Experimental setup for free carrier absorption measurements.

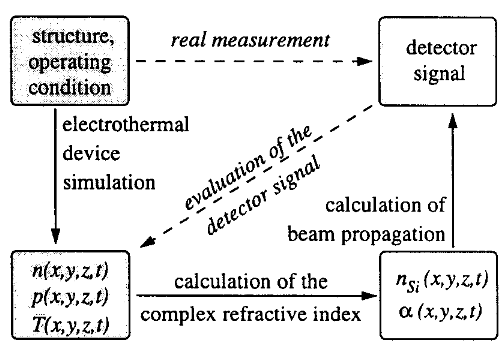

Fig. 2. Strategy for the simulation of internal laser probing techniques.

0-7803-6279-9/00/$10.00 © 2000 IEEE

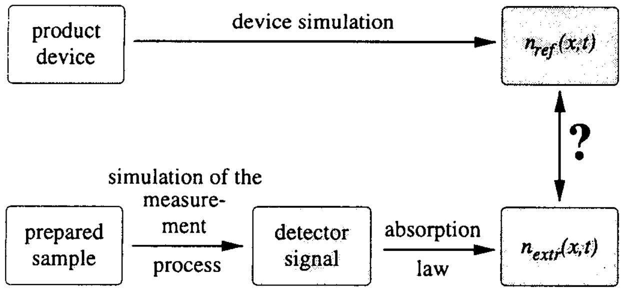

Fig. 3. Employing virtual experiments to optimize free carrier absorption measurements.

follow the strategy illustrated in Fig. 2:

The first step consists of an electrothermal device simulation [4] from which we obtain the transient carrier density and temperature profiles. From these data the modulations of the complex refractive index are calculated. Finally, simulating the beam propagation through the sample, the lenses, and aperture holes yields the calculated detector signal.

III. Virtual Experiments

The real measurements can only be carried out on properly prepared samples of suitable size. Additionally, their surfaces have to be polished which enhances the surface recombination rate. On the other hand, device engineers are interested in the carrier distribution within unprepared product devices. Therefore, the goal of an optimized experiment is that the effects due to the sample preparation and the measurement process itself are negligible and the measured carrier concentration profile reflects the carrier distribution within the product device.

Since the latter is accessible by simulation only, "virtual experiments" (cf. Fig. 3) are performed to optimize the experimental setup and to assess the accuracy of the optimized measurements. For that purpose, the carrier profile $n_{ref}(x,t)$ within unprepared product devices is calculated by an electrothermal device simulation and kept as a fixed reference during the optimization process. For different sample geometries and experimental setups, the measurement process is simulated, yielding a calculated detector signal. From this, in turn, a virtual carrier concentration $n_{extr}(x,t)$ is extracted from the absorption law (1) which would also be employed to evaluate the real measurements. Optimum probing conditions are attained if n_{extr} matches n_{ref} as close as possible.

IV. Optimizing the Sample Size

It is well-known that the experimental accuracy of free carrier absorption measurements on small samples is limited by surface recombination. In large dies, however, the spatial resolution suffers from the lateral spreading of the probing beam.

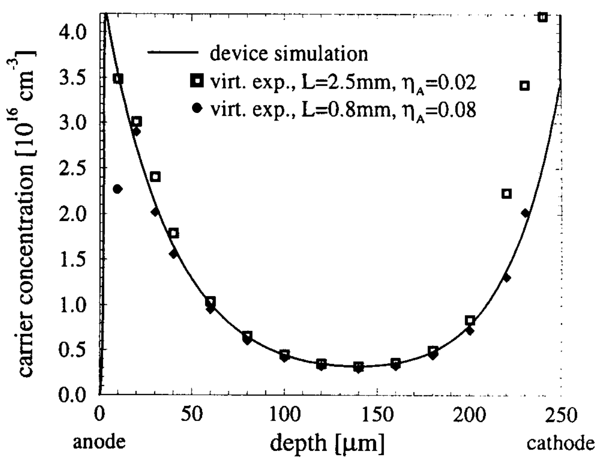

Fig. 4. Comparison of the carrier distribution within a power pin diode extracted from virtual absorption experiments on samples of different sizes.

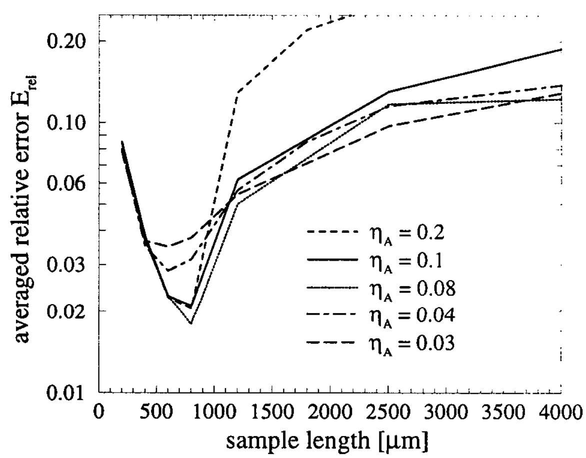

Fig. 5. Relative deviation of the carrier distribution extracted from a virtual experiment from the reference profile obtained by device simulation.

Consequently, there is an optimum sample length which minimizes the deviation of the extracted carrier concentration profile from the real carrier distribution (cf. Fig. 4). For a quantitative analysis, the average relative error E_{rel} is defined as

$$E_{rel} := \sqrt{\frac{1}{N}\sum_{i=1}^{N}\left(\frac{n_{extr}(x_i)}{n_{ref}(x_i)} - 1\right)^2} \tag{2}$$

where N denotes the number of measured sampling positions x_i.

Carrying out virtual experiments on devices with a carrier lifetime of $0.8\,\mu$s reveals an optimum sample length of

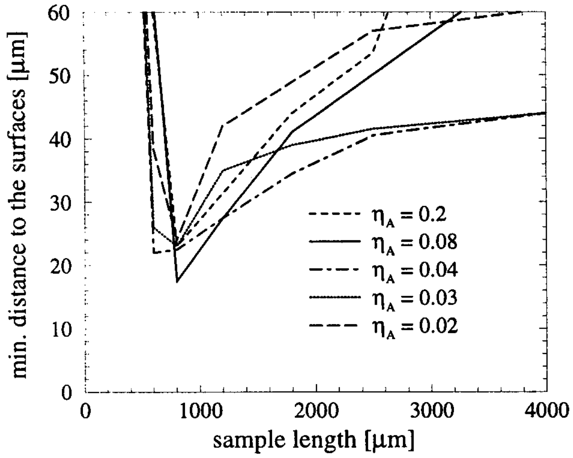

Fig. 6. Minimum distance which has to be kept to the device's top and bottom surfaces.

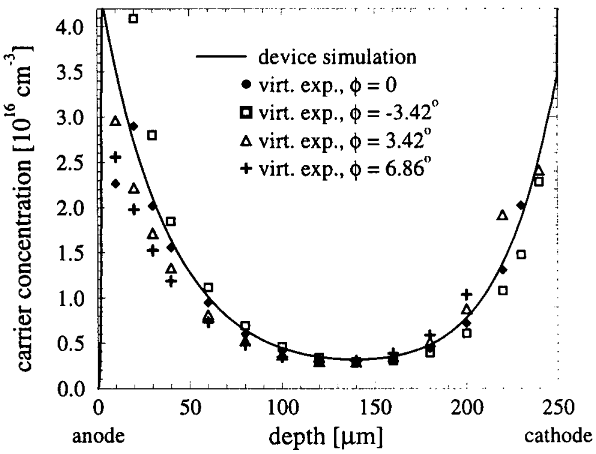

Fig. 7. Comparison of the carrier concentration profile for absorption measurements with non–normal incidence.

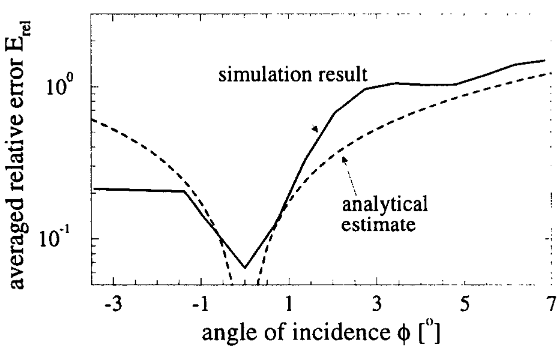

Fig. 8. Relative error for non–normal incidence.

800 μm, i. e. 20 diffusion lengths. Choosing the angular aperture η_A of the probing beam accordingly, the deviation of the extracted concentration from the reference distribution can be reduced to only a few percent (cf. Fig. 5). Virtual experiments for different values of the carrier lifetime (figures not shown) also suggest an optimum sample length of 20 diffusion lengths. In this case, as well, an error of only a few percent can be attained.

Since reflections off the metallization layers at the anode and cathode significantly distort the beam profile and thus corrupt the measurement signal, only part of the bulk region of the device interior can be investigated properly. Optimizing the sample geometry also facilitates measurements closer to the top and bottom device surfaces. A quantitative investigation is shown in Fig. 6, where the necessary minimum distance to the device surfaces has been defined by the position x_i where the relative error $n_{extr}(x_i)/n_{ref}(x_i) - 1$ exceeds 10 %.

V. Sample alignment

In the previous sections, normal incidence of the laser beam on the side face of the device has been assumend. However, an oblique transition of the probing beam into the device has a sensitive influence on the averaged interaction with the carriers along the optical path. Fig. 7 and 8 illustrate the error due to non–normal incidence of the probing beam. The numerical results from the rigorous model are compared with a simple analytical estimate. It is based on the average carrier concentration along a beam path tilted by an angle Θ in the interior of the device

$$E_{rel,anal} = \sqrt{\frac{1}{N}\sum_{i=1}^{N}\left(\frac{\int_0^L n(x+z\tan(\Theta),z)\,dz}{n_{ref}(x)\cdot L} - 1\right)^2} \tag{3}$$

where Θ is related to the angle of incidence Φ by the refraction law.

However, due to temperature–induced gradients of the refractive index, an additional internal deflection gives rise to a curved propagation of the probing beam. Therefore, the numerical result is not symmetric with respect to $\Theta = 0$. Nevertheless, together with the analytical estimate it clearly demonstrates that a non–vanishing angle of incidence can easily introduce an error of several 10 %. An accurate sample alignment therefore constitutes a decisive precondition for precise and reliable measurements results.

VI. Application Example

The measured carrier distribution in the interior of power devices provides valuable information for calibrating a numerical device simulator and for optimizing the device performance. As an example to demonstrate the benefit of absorption measurements, the carrier distributions in the interior of a high voltage diode at different current densities were investigated. The excellent capabilitities of the optimized experimental setup are reflected in the smooth profiles which, e. g., facilitate a precise extraction of the carrier lifetime. These data were used to calibrate the carrier lifetime model of a general purpose device simulator [4]. Thus, a generally valid set of parameters for this kind of device technology can be found which accurately reproduces the carrier distribution at all current densities (cf. Fig. 9).

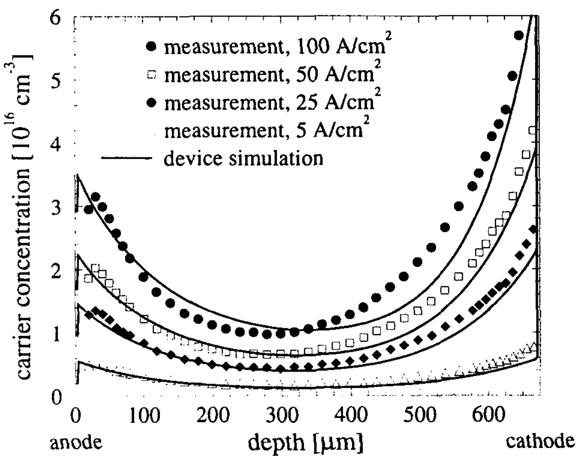

Fig. 9. Carrier distribution for various current densities.

VII. Conclusion

We have presented a comprehensive analysis of free carrier absorption measurements which includes the effects due to the sample preparation and the measurement process itself. A physically rigorous simulation strategy of the entire measurement process has been employed to carry out "virtual experiments". Quantitative results for the optimum sample geometry and the corresponding angular aperture of the probing beam have been obtained and the effects of a possible misalignment of the device under test have been investigated. In summary, we conclude that the simulation of the complete measurement process constitutes a valuable methodology to identify and to tackle the most significant sources of error and to assess the accuracy of the optimized experiments.

References

[1] H. B. Briggs, R. C. Fletcher, "Absorption of Infrared Light by Free Carriers in Germaninum," Physical Review Vol. 91, No. 6, 1342, (1953)

[2] R. W. Cooper, D. H. Paxman, "Measurement of charge-carrier behaviour in pin diodes using a laser technique," Solid State Electronics, Vol. 21, 865, (1978)

[3] R. Thalhammer, F. Hille, G. Wachutka, "Numerical Simulation of Infrared Laser Probing Techniques," Proc. of SISPAD, Leuven, Belgium, 276, (1998)

[4] R. Escoffier, U. Krumbein, E. Lyumkis, B. Polsky, A. Schenk, B. Schmithüsen, C. Steiner, W. Fichtner, "DESSIS 4.0 Manual," DESSIS 4.0 Manual, ISE Integrated Systems Engineering AG, Zurich, CH, (1996)